The AAPS Journal, Vol. 19, No. 1, January 2017 (© 2016)
DOI: 10.1208/s12248-016-9978-y

Research Article

Theme: Next Generation Formulation Design: Innovations in Material Selection and Functionality
Guest Editors: Otilia M. Koo, Panayiotis P. Constantinides, Lavinia M. Lewis, and Joseph Reo

The Effect of Polymorphism on Surface Energetics of D-Mannitol Polymorphs

Robert R. Smith,[1] Umang V. Shah,[1] Jose V. Parambil,[1] Daniel J. Burnett,[2] Frank Thielmann,[3] and Jerry Y. Y. Heng[1,4]

Received 26 April 2016; accepted 17 August 2016; published online 8 September 2016

Abstract. The aim of this work was to assess the effect of different crystalline polymorphism on surface energetics of D-mannitol using finite dilution inverse gas chromatography (FD-IGC). Pure α, β and δ polymorphs were prepared via solution crystallisation and characterised by powder X-ray diffraction (P-XRD). The dispersive surface energies were found to range from 43 to 34 mJ/m^2, 50 to 41 mJ/m^2, and 48 to 38 mJ/m^2, for α, β, and δ, respectively, for surface coverage ranging from 0.006 to 0.095. A deconvolution modelling approach was employed to establish their energy sites. The primary sites corresponded to maxima in the dispersive surface energy of 37.1 and 33.5; 43.3 and 39.5; and 38.6, 38.4 and 33.0; for α, β, and δ, respectively. This methodology was also extended to an α-β polymorph mixture to estimate the amount of the constituent α and β components present in the sample. The dispersive surface energies of the α-β mixture were found to be in the range of 48 to 37 mJ/m^2 with 40.0, 42.4, 38.4 and 33.1 mJ/m^2 sites. The deconvolution modelling method extracted the energy contribution of each of the polymorphs from data for the polymorphic mixture. The mixture was found to have a β-polymorph surface content of ~19%. This work shows the influence of polymorphism on surface energetics and demonstrates that FD-IGC coupled with a simple modelling approach to be a powerful tool for assessing the specific nature of this energetic distribution including the quantification of polymorphic content on the surface.

KEY WORDS: D-mannitol; inverse gas chromatography; modelling; polymorphism; powder X-ray diffraction; surface energy heterogeneity.

INTRODUCTION

Materials of pharmaceutical interest exhibit polymorphism, which can have a direct effect on many aspects of product performance, such as bioavailability (1) and efficacy (2), and on physical properties, such as transition temperature (3) and surface free energy (4). Solid dosage forms are usually formulated with the thermodynamically most stable forms of API and excipients. However, metastable polymorphic form is occasionally preferred over the stable form in case of improved materials handling, flowability, compaction/tableting, or dissolution. Product behaviours such as flowability (5–7), mixing (8), compactability (9) and dissolution rates (10) are assisted by interfacial interactions between particles. Hence, if different polymorphs of a material are to be used for formulation, it would be very important to investigate surface energy heterogeneity of these polymorphs as it governs interfacial behaviour between materials.

Surface energy of pharmaceutical materials, both active ingredients (11, 12), and excipients has been demonstrated to be anisotropic (13). Facet specific surface energy of crystalline pharmaceutical material was directly correlated with the presence of functional end groups of the facets. Considering the facet specific surface energy for a pharmaceutical material, it is reported that surface energetics of a crystalline powder depends on relative contribution of different crystal facets (14). Crystals of same polymorphic forms, but different crystal shapes, have been studied to understand role of crystal habits on surface energetics. Shah et al. correlated changes in surface energy of different crystal habits of an anti-inflammatory drug with the varying contribution of different crystal facets (14).

Although the surface energetics of crystalline systems have been extensively investigated in the last decade, the

[1] Surfaces and Particle Engineering Laboratory, Department of Chemical Engineering, Imperial College London, South Kensington Campus, London, SW7 2AZ, UK.
[2] Surface Measurement Systems Ltd., 2125 28th Street SW, Suite 1, Allentown, Pennsylvania 18103, USA.
[3] Novartis Pharma, Technical Operations, Schaffhauserstrasse, 4322, Stein, Switzerland.
[4] To whom correspondence should be addressed. (e-mail: jerry.heng@imperial.ac.uk), URL: http://www.imperial.ac.uk/spel

effect of polymorphism on surface energy heterogeneity is yet to be fully appreciated. The difficulty in crystallising pure crystals of different metastable polymorphic forms for surface energy heterogeneity measurements has been challenging (15). Solvent and humidity induced transformation of crystal forms and limited success in reproducibly preparing different polymorphs has hindered the progress. Recently, Cares-Pacheco, et al. have reported the surface energy heterogeneity of different polymorphic forms of D-mannitol (16). β and δ polymorphs of D-mannitol were reported to be energetically homogeneous, whereas α polymorphs was found to be energetically heterogeneous. Furthermore, surface energy differences between β and δ forms were reported to be non-significant compared to α form (16).

Polymorphic transformation of different compounds of pharmaceutical relevance, including mannitol, and its effect of manufacturability is well documented in the literature (17). Information on solid-state structure of the polymorphic forms has allowed predicting its mechanical properties (18). Such capabilities have allowed the prediction of particulate compaction, or breakage behaviour in case of polymorphic transformation. Moisture induced polymorphic transformation of the δ-form to the β-form is known to result in substantial morphological changes, ultimately resulting in the significant increase in specific surface area. Such behaviour was attributed to the presence of water molecules disrupting the H-bonds of mannitol, followed by an instantaneous reconstruction of H-bond network to form the thermodynamically stable β form (19). Furthermore, considering anisotropy in mannitol crystals (13), as a result of polymorphic transformation, functional end groups exposed on the surface may result in a change in the surface energetics of the mannitol powders. Such changes in surface energetics in addition to changes in shape ultimately affect its powder flow properties, i.e. cohesion, ultimately effecting manufacturability (14).

This study aims to develop an approach to determine the surface energy heterogeneity of polymorphs and to employ a deconvolution modelling approach to determine surface energy distributions. Such an approach is aimed at quantifying the surface composition of polymorphic mixtures, opening up new avenues of polymorphic mixture quantification using surface energy heterogeneity measurements.

THEORY

The principle technique employed in this study is that of finite dilution inverse gas chromatography (FD-IGC). This technique is a method for measuring the surface energy heterogeneity (distribution of surface energy due to different active sites) of materials and is an extension of the commonly employed infinite dilution inverse gas chromatography (ID-IGC).

Infinite Dilution Inverse Gas Chromatography

The theory of IGC for use in dispersive surface energetic calculations first starts with the dispersive work of adhesion between an interface as defined by Fowkes (20) below:

$$W_a^d = W_{c,1}^d + W_{c,2}^d = 2\left(\gamma_1^d \gamma_2^d\right)^{\frac{1}{2}} \quad (1)$$

Where, $W_a{}^d$ is the dispersive work of adhesion, $W_{c,1}{}^d$ and $W_{c,2}{}^d$ are the work of cohesion at the interface of phase 1 and 2, respectively, and $\gamma_1{}^d$ and $\gamma_2{}^d$ are the dispersive surface free energies of the two phases.

Further, it can be shown that the Gibbs free energy of adsorption can be equated directly with this work of adhesion by the following:

$$-\Delta G_{ad}^d = N_a \cdot a_m \cdot W_a^d \quad (2)$$

Where $G_{ad}{}^d$ is the dispersive component of the Gibbs free energy of adsorption, N_a is Avogadro's number and a_m is the cross-sectional area of an incident liquid molecule.

The Gibbs free energy can then be related to a quantity directly measurable by IGC, the retention volume, in the following way:

$$-\Delta G_{ad}^d = RT\ln V_N + K \quad (3)$$

Where R is the universal gas constant, T is the temperature of the column, V_N is the retention volume and K is a constant dependent on the reference state of the system.

The retention volume is defined as the volume of carrier gas required to remove an adsorbate from an adsorbed state on an adsorbent. This can be calculated by IGC using the retention time of the solvent as in the relation below:

$$V_N = \frac{j}{m} F(t_r - t_0) \frac{T}{T_{Ref}} \quad (4)$$

Where j is the James-Martin pressure drop correction factor, t_r is the retention time of the interacting species, F is the flow rate of the carrier gas, t_0 is the dead time of a non-interacting species, and T_{Ref} is the reference temperature. With rearrangement of Eqs. (1) to (3), and as defined, we obtain the following relation.

$$RT\ln V_N + K = N_a \cdot a_m \cdot 2\left(\gamma_1^d \gamma_2^d\right)^{1/2} \quad (5)$$

There are other proposed modalities to this illustrated here, such as the employment of a harmonic mean rather than a geometric mean as proposed by Wu (21). However, for the purposes of this study, only the commonly applied geometric mean will be used. Further, the choice of cross-sectional surface area and surface free energy of the solvent used is a point of contention and various methodologies may be employed. The approach utilised here for simplicity is that of the Schultz approach (22), the most pertinent alternate approach to mention is that of the Dorris-Gray approach (23), which uses the surface energy and cross-sectional areas of a single methylene group yielding a linearly increasing trend with increasing n-alkane chain length. The choice here has been shown to provide only slight differences in energy values calculated (24), and the impact on this study will be discussed further at a later point.

Finite Dilution Inverse Gas Chromatography

The approach discussed so far is the basics of measuring dispersive surface free energy of a material; it is intended to be used only at infinite dilution that is low concentration injections of the alkane probes discussed. This approach yields energetic values that are typically higher than the average surface free energy of the material. Further, this approach yields a singular value for the material, when in reality, most materials exhibit a degree of heterogeneity, whether chemical or by structural inhomogeneity/defects (25) and so a solution providing information on this heterogeneity is required. Initial approaches to this yielded either system specific information (26) or limiting assumptions about the physical process described (27). However, later approaches were made which provided system independent information about materials, with data comparable with alternative techniques and far more descriptive of the surface investigated. This approach is to conduct identical analysis as previously discussed, but over a range of concentrations, to provide information about the system at varying surface coverage, so providing a more complete picture of the material of interest.

The number of moles adsorbed for a given injection of solvent can be found using the following relation:

$$n = \frac{1}{RT_{col}m}\int V_N dP \tag{6}$$

where n is the number of moles, m is the mass of the sample and P is the equilibrium partial pressure. The equilibrium partial pressure is the reduced partial pressure experienced at equilibrium within the column, due to various effects such as peak broadening and temperature considerations. It can be calculated from the following:

$$P = \frac{h}{F.A}\cdot V_{loop}\cdot\frac{T_{Ref}}{T_{Loop}}\cdot P_{inj} \tag{7}$$

where, h and A are the height and area of the chromatogram, respectively, V_{loop} is the volume of the injection loop, T_{loop} is the temperature of the loop, T_{Ref} is the reference temperature and P_{inj} is the partial pressure of the solvent injected.

This can then be used to calculate an adsorption isotherm, which in turn may be analysed in the manner delineated by Brunauer-Emmett-Teller (28) to calculate a 'monolayer surface coverage' molar quantity, n_m. By taking the number of moles of a given injection and comparing it to the monolayer capacity, one can find the fractional surface coverage. This allows for a surface energy analysis of the manner described previously to repeat at multiple coverages, yielding an energetic distribution (29).

Expanding further from FD-IGC, Jefferson et al. modelled the adsorption process by employing thermodynamic considerations, yielding a discretised energetic map, to better understand the specific contributions involved (30).

Modelling Approach

The information provided by the experimental methods discussed so far yield some insights into a material's characteristics. However, they imply a continuum of energies for a given system, which can be seen as being an inaccurate view of real materials as can be seen by direct analysis of materials with other techniques. As such, a method of extracting more discretised information about the system is necessary. To this end, a modelling approach which simulates the energetic distributions as calculated by the FD-IGC methodology, yielding information on discrete energetic contributions and their relative proportions has been developed previously and will be outlined below, a full explanation can be found elsewhere (31).

Figure 1 shows the step by step process of modelling approach adopted in this study. The probability of relative adsorption events are described by the Boltzmann distribution for the various sites with a given solvent, using the adsorption potential, as described below:

$$\frac{N_i}{N} = \frac{e^{\left(-\Delta G^{d}_{adi}\middle/ k_B T\right)}}{\sum_i e^{\left(-\Delta G^{d}_{adi}\middle/ k_B T\right)}} \tag{8}$$

where $\frac{N_i}{N}$ describes the probability of being in state i, given a population of states N, $-\Delta G_{adi}{}^{d}$ is the adsorption potential associated with state i and k_B is the Boltzmann constant (Fig. 1a shows the probability of adsorption of a n-heptane molecule on a particular energy site).

The energy of independent sites of a material is then modelled as being normally distributed around a given value, as has been shown by alternative techniques (32), using the standard result for the normal distribution as shown below:

$$f\left(\gamma_S^d\right) = \frac{1}{\sigma\sqrt{2\pi}}e^{\frac{1}{2}\left(\frac{\gamma_S^d-\mu}{\sigma}\right)^2} \tag{9}$$

where μ is mean value of the surface energy, i.e. the value ascribed as the surface energy for a given site, σ is the standard deviation, which for a normally distributed function is 1 and all other symbols have their usual meaning.

The product of these two components normalised to a value of 1 provides the relative overall probability of an adsorption event taking place. Relative filling of sites in incremental coverage can be ascribed by the probability (Fig. 1b shows the referred concept). However, after an adsorption event occurs, the number of sites remaining for adsorption decreases. This can be seen to more strongly affect the sites with higher adsorption probability. As such, a new distribution is created, the product of this and the Boltzmann distribution as described then provides a new probability for adsorption. This process can be repeated until all sites are occupied by an iterative process, yielding an overall energetic occupation for a given material and solvent (an example of the effect on relative occupancy of sites for n-heptane is shown in Fig. 1c.). This process is then repeated for each solvent used in the experimental system, the energies 'experienced' by each solvent is then back calculated to an

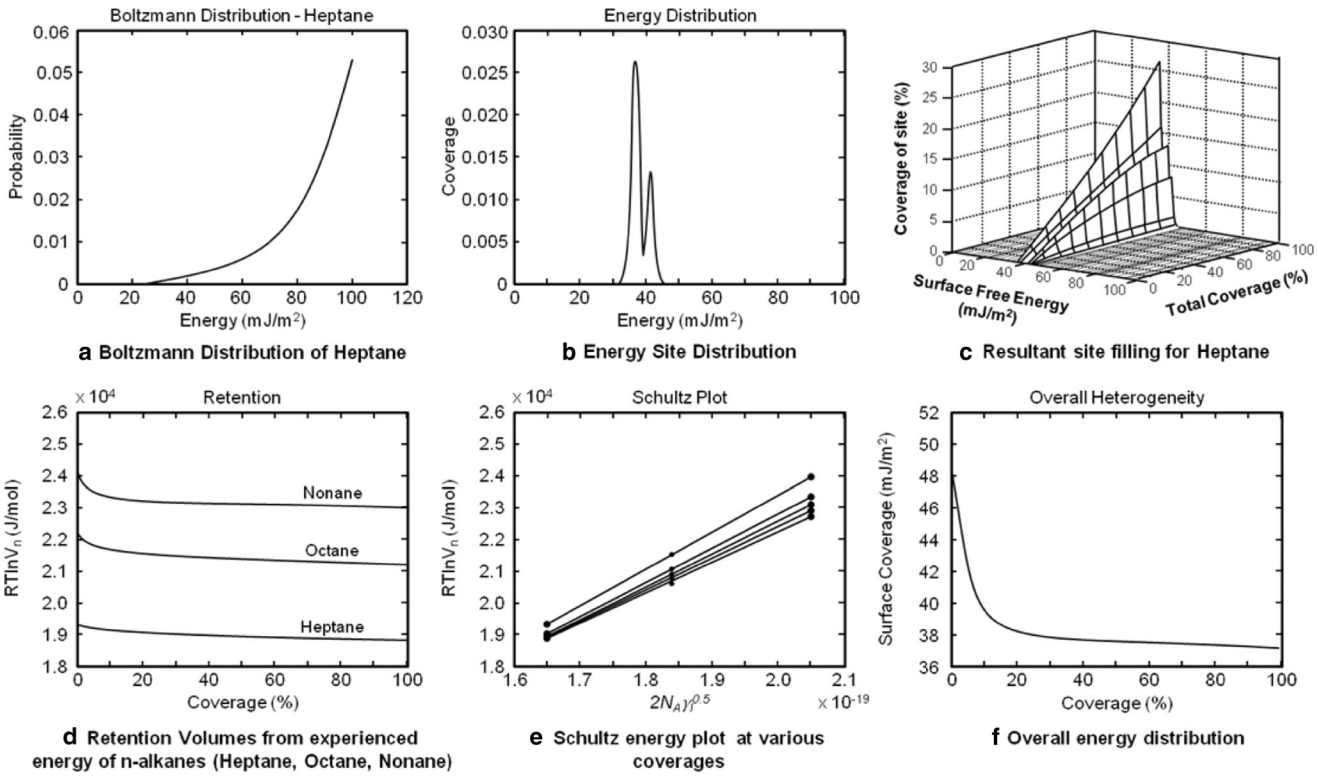

Fig. 1. The modelling procedure for surface energy deconvolution; **a** Boltzmann distribution showing the n-heptane probability of adsorption of a molecule on a particular energy site, **b** probabilistic weightings of the site filling by the relative number weighting of the relative energy sites (normalised to 1), **c** changes in relative site occupancy with changing coverages, **d** calculated retention volumes as a function of surface coverage for different alkanes, **e** the Schultz plot for the corresponding retention volumes computed for various surface coverages, **f** the surface energy distribution calculated from the Schultz plot.

'experienced' retention volume (Fig. 1d shows 'experienced' retention volumes for heptane, octane, and nonane), which can then be examined by identical analysis procedures as the experimental data (i.e. Schultz and Dorris-Gray). Figure 1e shows calculated Schultz plot for retention volumes calculated at different surface coverages (Fig. 1c), which can be compared with experimental data for validation. From the calculated Schultz plot, resultant energy distribution can be calculated using the Schultz method on the basis of computed retention (Fig. 1f).

EXPERIMENTAL METHODS

Crystallisation of D-mannitol Polymorphs

Pure α- mannitol was produced by dissolving mannitol in water at 60–65°C and crashed out of solution using cold acetone as an anti-solvent. Pure β form is prepared from a 40 *w*/*w*% mannitol in water dissolved at 60–65°C and allowed to cool to room temperature whilst stirred for 24 h. δ-form is prepared via evaporative crystallisation of 40 *w*/*w*% mannitol solution in water as described by Poornachary et al. (33) and δ crystals that grew out from the solution interface were carefully removed and analysed/stored.

Powder X-Ray Diffraction (PXRD)

PXRD (X'Pert Pro Diffractometer, PANalytical B.V., Almelo, The Netherlands) was employed to confirm the polymorph present within the samples. PXRD was collected over the range of 5–40° 2θ with a CuKα X-ray source at 40 kV and 40 mA. The data obtained was compared to that from the materials database as well as with the literature to ascertain the polymorphism of the material.

Inverse Gas Chromatography

All FD-IGC experiments were performed with an SEA-IGC (Surface Measurement Systems Ltd., London, England). Samples were first conditioned with helium at 30°C at a flow rate of 10 sccm for 20 min. Subsequently, an n-nonane isotherm was measured to determine the sample surface area. Following this, to measure dispersive component of surface energy, n-heptane, n-octane and n-nonane were injected with target n/n_m values of 0.006, 0.009, 0.01, 0.02, 0.03, 0.04, 0.05, 0.06, 0.07, 0.08, 0.09 and 0.12. This procedure was repeated three times for reproducibility. For calculation of dispersive component of surface energy, two different methods, Schultz and Dorris-Gray, are reported in the literature. Out of the two methods, the Schultz method is one of the established methods for calculation of dispersive surface energy and has been widely used. Shi et al. compared the Dorris-Gray and Schultz methods for calculation of surface energies and reported the differences in dispersive surface energy calculated as a function of temperature (24). It is reported that at higher measurement temperatures, the Schultz method can underestimate dispersive component of surface energy compared to the Dorris-Gray method. It can

also be observed from the literature that although absolute dispersive surface energy values may differ for two different calculation methods, trend in surface energy for different material is similar (24, 34). However, at 30°C, which is also the measurement temperature in the current study, dispersive surface energy calculated by the Schultz and Dorris-Gray methods was found to be very similar (24). Considering the evidence that dispersive surface energy calculated by both the Schultz and Dorris-Gray methods is very similar at measurement temperatures of this study, to calculate dispersive component of surface energy, widely used method reported by Schultz et al. was used (22). No energy value was used for the purposes of this study whose Schultz plot did not provide an $R^2 > 0.999$, as this is a suggested measure of the quality of utilisable data for FD-IGC (35). Each measurement repeated at least three times for reproducibility.

RESULTS AND DISCUSSION

Characterisation of D-mannitol Polymorphs

Powder X-ray diffractograms for all three polymorphs of D-mannitol, as well as polymorphic mixture of metastable form α, and thermodynamically stable form β are shown in Fig. 2. Polymorphic identity of the crystals obtained in this study was confirmed by comparing the PXRD pattern of different crystals obtained in this study with the predicted diffraction patterns that were generated using *Reflux* module in Materials Studio 5.5 (Accelrys Software Inc.). Furthermore, PXRD patterns obtained in this study for different polymorphs of D-mannitol was also compared with literature confirming the presence of all three different polymorphs of D-mannitol (16, 33). The powder pattern of α polymorph was characterised by peaks at 2θ values 9.5°, 13.8°, and 17.4°. The δ polymorph was distinguished with a prominent peak at 2θ value 9.7° and absence of any peak until 19.5°. The characteristic peaks for the stable β form is seen at 2θ values of 14.8° and 16.9° with a relatively small peak at 10.6°. As can be seen from Fig. 2, that all three forms, α, β, and δ polymorphs exhibit only the characteristic peaks confirming the purity of polymorphs. However, the diffraction pattern for mixture of α and β exhibits peaks which correspond with those characteristic of the α, as well as β polymorphs, implying that a some β polymorph is present within the sample α. Though the accurate quantification of polymorphic mixture cannot be determined by this method alone and further calibration and analysis is required to quantify composition involving pure α and β forms from PXRD results.

PXRD is the definitive technique which is one of the most widely used techniques for quantification of polymorphic mixtures (36). However, PXRD is simple in measurement, and it suffers with low resolution (limited accuracy >5%) and inability to differentiate between surface/bulk composition of crystalline mixture (37). Considering that surface energy heterogeneity measurements using FD-IGC only probes the surface, if employed for polymorphic composition determination, it can provide comparatively higher resolution and can quantify any surface polymorphic transformations.

Surface Energy Heterogeneity of D-mannitol Polymorphs

Experimentally determined dispersive surface energy distributions for all three polymorphs of mannitol, as well as that of α-β mixture by FD-IGC, are shown in Fig. 3. As can be seen, β polymorph possesses the highest energy ranges from around 51 to 41 mJ/m^2 from low to high surface coverage. This is followed by the δ form with surface energy values from 49 to 38 mJ/m^2 and the α form is found to exhibit lowest surface energy, ranging from 43 to 34 mJ/m^2, for surface coverage ranging from $n/n_m = 0.006$ to 0.095.

The mixture of α-β is found to exhibit the surface energy between that of pure α-form and pure β-form. Surface energy for polymorphic mixture ranges between 49 and 37 mJ/m^2. The explicit contribution from α can be inferred as being the lowest of the three polymorphs, given the lowest energy expressed by a mixture of it and an otherwise more energetic polymorph. In contrast to a recent literature (16), surface energetics of each polymorph are shown to descend in an order of $\beta > \delta > \alpha$. The difference here can be attributed to the dissimilar approach taken to determine surface energy heterogeneity and the difficulty in preparation and characterisation of pure α. To further validate experimental findings, a

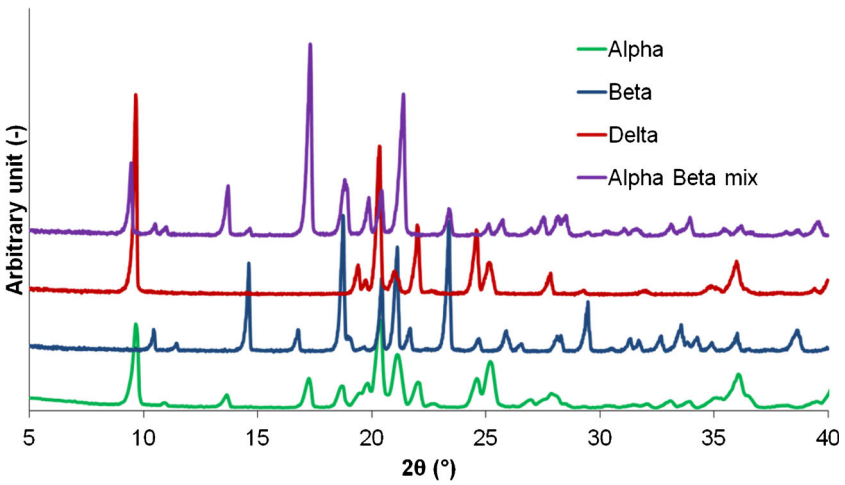

Fig. 2. PXRD patterns of the various polymorphic forms of D-mannitol; α, β, and δ, and α-β mix.

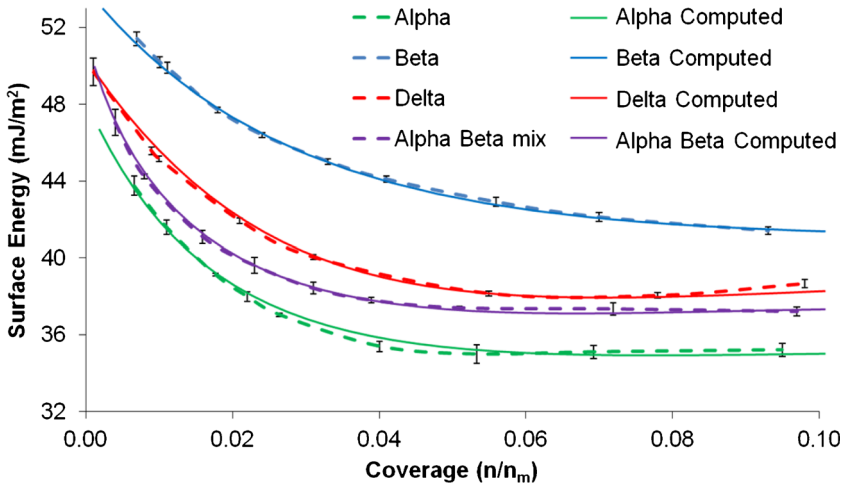

Fig. 3. Experimentally determined surface free energy distributions (*dotted lines*) and those calculated by the modelling procedure (*continuous lines*) outlined, for the various polymorphic forms of D-Mannitol.

computational approach is adopted in this study to separate explicit contribution of α from the polymorphic mixture of α and β (conventionally crystallised polymorphic mixture) and discussed in the *section* Computational Approach to Predict Surface Energy Heterogeneity of Metastable Form, and Quantification of Polymorphic Mixture.

Computational Approach to Predict Surface Energy Heterogeneity of Metastable Form, and Quantification of Polymorphic Mixture

The modelled data for the FD-IGC is shown overlaid with that measured experimentally in Fig. 3. The computed values agree very well with experimental data, with each having a $\chi^2 < 0.9$, this metric describes the closeness of fit as the sum of the squares of differences between the measured and calculated distributions.

Figure 4 shows main dispersive energy components determined for each of the α, β, δ polymorph and the relative mix of α-β forms. The implied energetic values for the β polymorph matches well with expectations which can be drawn from other, alternate measurement technique (13), with major energetic sites 43.3 and 39.5 mJ/m^2 with weightings of 39.5 and 60.0%. The δ polymorph is seen to be primarily dominated by a single peak, which is actually the product of two very similarly valued energy sites, with values of 38.6 and 38.4 mJ/m^2 and weightings of 39.1 and 57.1%, respectively, which can be considered as a single energetic contribution. This fairly singular value dominated distribution could be attributed to its needle-shaped crystals obtained for δ form. However, a smaller but significant energy site can be seen centred around 33.0 mJ/m^2 with a weighting of 3.6%. Pure α was observed to contain major energetic sites of 37.1 and 33.5 mJ/m^2, with weightings of 17.1 and 82.7%, respectively.

The mixture of α and β was found to have a major energy site at 33.1 mJ/m^2 with a weighting of 81.2%. A significant contribution to the overall energetic profile of this mixture is found to exist in the region of the characteristic peaks of the β polymorph, at 40.0 mJ/m^2, 42.4 mJ/m^2 and a smaller peak at 38.4 mJ/m^2, with weightings of 9.8, 7.2 and 1.7%, respectively, given this weighting an apparent total contribution to the energy for the mixture of ≈19%, which in turn implies a 19% surface area contribution by the β polymorph to the overall mixture. The beta form is present on the surface of a particle made up of the alpha form, based on XRD data (Fig. 2). Each distribution was found to also contain a small higher energy fraction, with weightings

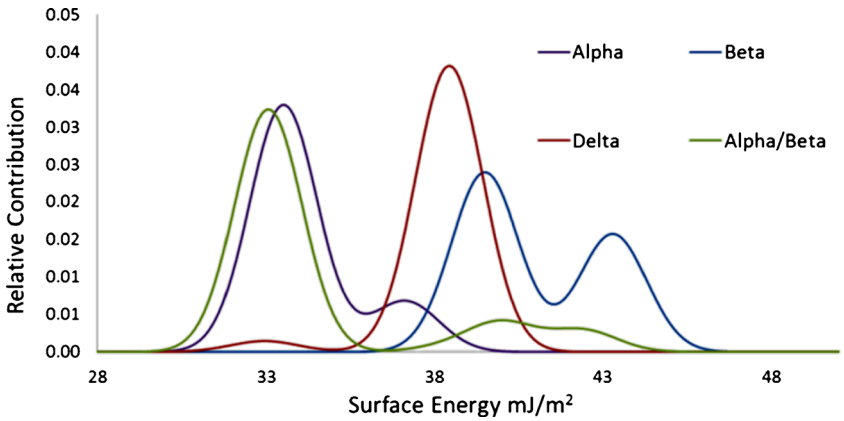

Fig. 4. The main energy components determined for each of the α, β, δ polymorph and the relative mix of α-β.

<0.1%. Figure 4 shows the major energetic contributions of each of the polymorphs.

When the free energy distribution of the α-β mixture is compared to that of pure α and pure β (Fig. 3), an apparent deviation of the free energy distribution of the mixture is observed at low surface coverages. However, when the actual distribution of sites is made in the α-β mixture (Fig. 4), the major contributing component can be seen as remarkably similar, with the de-convoluted alpha having a major component at 33.1 mJ/m^2 and that from a pure sample having its major component at 33.5 mJ/m^2. The notable difference between the two is a relatively substantial contribution at 37.1 mJ/m^2 for pure α which is not seen in the distribution for α-β mixture. This could be a result of many different factors, including any size differences resulting from the different growth rates of pure alpha and the alpha in the polymorphic mixture with beta.

This study reports on an approach to investigate the surface energetics of a metastable and difficult to crystallise polymorph compared to the surface energy heterogeneity measurements of a stable polymorph, and a binary mixture of target polymorph with stable polymorph. A modelling approach to deconvolute the contribution of each polymorphic component is reported, to estimate the proportion of the said polymorphic form on the surface of the particles. Where other techniques (e.g. XRD) are employed, the results may not be in good agreement, as these 'orthogonal techniques' would provide a bulk quantification of the polymorph and not the surface. It may be possible to utilise other specialised spectroscopic techniques, though this is beyond the scope of the study.

CONCLUSION

The different polymorphic forms of D-mannitol have been observed as exhibiting distinct surface energetic properties as would be expected. The specific energetics of each polymorph are shown to descend in an order of $\beta > \delta > \alpha$, with the profiles exhibiting dispersive surface energy ranges of 50 to 41 mJ/m^2, 48 to 38 mJ/m^2 and 43 to 34 mJ/m^2, respectively. Further, the modelling approach applied was able to define a suggested surface contribution of ~19% of the β polymorph in a mixture of undetermined constitution. A computationally constructed relative energy distribution for metastable α polymorph was determined from the mixture of α and stable form β which agreed well with the experimental values obtained. In summary, findings of this study demonstrate an approach to predict surface energetics of a metastable/difficult to crystallise polymorph from surface energy heterogeneity measurements of a stable polymorph, and a binary mixture of target polymorph with stable polymorph. Such approach is not only limited to demonstrate prediction of surface energy heterogeneity profile for a polymorph difficult to crystallise in pure form, but also employed to calculate composition of a binary polymorphic mixture, opening up avenues for quantification of polymorphic mixtures employing surface energy heterogeneity measurements.

ACKNOWLEDGMENTS

The PhD studentship, supported by the Engineering and Physical Science Research Council and Surface Measurement Systems for Robert Smith, is gratefully acknowledged.

REFERENCES

1. Aguiar AJ, Krc J, Kinkel AW, Samyn JC. J Pharm Sci. 1967;56(7):847–53.
2. Borka L, Haleblian JK. Acta Pharm Jugosl. 1990;40:71–94.
3. Burger A, Ramberger R. Microchim Acta. 1979;72(3–4):259–71.
4. Navrotsky A. Geochem Trans. 2003;4(6):34.
5. Li Q, Rudolph V, Weigl B, Earl A. Int J Pharm. 2004;280(1–2):77–93.
6. Shah UV, Olusanmi D, Narang AS, Hussain MA, Tobyn MJ, Heng JYY. Int J Pharm. 2014;475(1–2):592–6.
7. Shah UV, Olusanmi D, Narang AS, Hussain MA, Tobyn MJ, Hinder SJ, et al. Pharm Res 2014: 1–12.
8. Das SC, Zhou Q, Morton DAV, Larson I, Stewart PJ. Eur J Pharm Sci. 2011;43(4):325–33.
9. Fichtner F, Mahlin D, Welch K, Gaisford S, Alderborn G. Pharm Res. 2008;25(12):2750–9.
10. Szekely J, Stanek V. Chem Eng Sci. 1969;24(1):11–24.
11. Heng JYY, Bismarck A, Lee AF, Wilson K, Williams DR. J Pharm Sci. 2007;96(8):2134–44.
12. Heng JYY, Bismarck A, Lee AF, Wilson K, Williams DR. Langmuir. 2006;22(6):2760–9.
13. Ho R, Hinder SJ, Watts JF, Dilworth SE, Williams DR, Heng JYY. Int J Pharm. 2010;387(1–2):79–86.
14. Shah UV, Olusanmi D, Narang AS, Hussain MA, Gamble JF, Tobyn MJ, *et al*. Int J Pharm. 2014;472(1–2):140–7.
15. Chemburkar SR, Bauer J, Deming K, Spiwek H, Patel K, Morris J, *et al*. Org Process Res Dev. 2000;4(5):413–7.
16. Cares-Pacheco MG, Vaca-Medina G, Calvet R, Espitalier F, Letourneau JJ, Rouilly A, *et al*. Int J Pharm. 2014;475(1–2):69–81.
17. Lee AY, Erdemir D, Myerson AS. Annu Rev Chem Biomol Eng. 2011;2(1):259–80.
18. Chattoraj S, Shi L, Sun CC. CrystEngComm. 2010;12(8):2466–72.
19. Yoshinari T, Forbes RT, York P, Kawashima Y. Int J Pharm. 2002;247(1–2):69–77.
20. Fowkes FM. Dispersion force contributions to surface and interfacial tensions, contact angles, and heats of immersion. Contact Angle, Wettability, and Adhesion. Advances in Chemistry. 43: American Chemical Society, 1964. p. 99–111.
21. Wu S. Macromol Sci C. 1974;10(1):1–73.
22. Schultz J, Lavielle L, Martin C. J Adhes. 1987;23(1):45–60.
23. Dorris GM, Gray DG. J Colloid Interface Sci. 1980;77(2):353–62.
24. Shi B, Wang Y, Jia L. J Chromatogr A. 2011;1218(6):860–2.
25. Buckton G, Gill H. Adv Drug Deliv Rev. 2007;59(14):1474–9.
26. Rudzinski W, Everett DH. Adsorption of gases on heterogeneous surfaces. London: Academic; 1992. p. 529–51.
27. Harris LB. Surf Sci. 1968;10(2):129–45.
28. Brunauer S, Emmett PH, Teller E. J Am Chem Soc. 1938;60(2):309–19.
29. Thielmann F, Burnett DJ, Heng JYY. Drug Dev Ind Pharm. 2007;33(11):1240–53.
30. Jefferson AE, Williams DR, Heng JYY. J J Adhes Sci Technol. 2011;25(4–5):339–55.
31. Smith RR, Williams DR, Burnett DJ, Heng JYY. Langmuir. 2014;30(27):8029–35.
32. Aubrey-Medendorp C. Atomic force microscopy method development for surface energy analysis [Doctoral Thesis]. Lexington, KY, United States: University of Kentucky; 2011.
33. Poornachary SK, Parambil JV, Chow PS, Tan RBH, Heng JYY. Cryst Growth Des. 2013;13(3):1180–6.
34. Gamble JF, Leane M, Olusanmi D, Tobyn M, Šupuk E, Khoo J, *et al*. Int J Pharm. 2012;422(1–2):238–44.
35. Ylä-Mäihäniemi PP, Heng JYY, Thielmann F, Williams DR. Langmuir. 2008;24(17):9551–7.
36. Stephenson GA, Forbes RA, Reutzel-Edens SM. Adv Drug Deliv Rev. 2001;48(1):67–90.
37. Shah B, Kakumanu VK, Bansal AK. J Pharm Sci. 2006;95(8):1641–65.